

Localized excitation in the hybridization gap in YbAl_3

J. M. Lawrence,¹ A. D. Christianson,^{1,3} E. A. Goremychkin,^{2,4} R. Osborn,² E. D. Bauer,³

J. L. Sarrao,³ J. D. Thompson³ and C. D. Frost⁴

¹University of California, Irvine, California 92697, USA

²Argonne National Laboratory, Argonne, Illinois 60439, USA

³Los Alamos National Laboratory, Los Alamos, New Mexico 87545, USA

⁴ISIS Facility, Rutherford Appleton Laboratory, Chilton, Didcot OX11 0QX, UK

The intermediate valence compound YbAl_3 exhibits a broad magnetic excitation with characteristic energy $E_1 \approx 50\text{meV}$, of order of the Kondo energy ($T_K \sim 600\text{-}700\text{K}$). In the low temperature ($T < T_{coh} \sim 40\text{K}$) Fermi liquid state, however, a new magnetic excitation arises at $E_2 \approx 33\text{meV}$, which lies in the hybridization gap that exists in this compound.

We show, using inelastic neutron scattering on a single-crystal sample, that while the scattering at energies near E_1 has the momentum (Q -) dependence expected for interband scattering across the indirect gap, the scattering near E_2 is independent of Q . This suggests that it arises from a spatially-localized excitation in the hybridization gap.

61.12.Ex, 71.28.+d, 75.20.Hr

The cubic (Cu_3Au structure) compound YbAl_3 exhibits strong intermediate valence ($z = 2.75$) and a large Kondo temperature ($T_K \sim 600\text{-}700\text{K}$). At high temperatures the behavior qualitatively follows the predictions of the Anderson impurity model but below the "coherence temperature" $T_{coh} \sim 40\text{K}$, the resistivity exhibits T^2 behavior and anomalies occur in the susceptibility, specific heat and Hall coefficient.¹ For $T < T_{coh}$ the optical conductivity² $\mathcal{S}_1(\omega)$ exhibits a narrow Drude peak separated by a deep minimum at 30meV from a mid-infrared peak at 0.25eV that arises from excitations across a hybridization gap. For $T > 40\text{K}$, $\mathcal{S}_1(\omega)$ broadens and tends towards normal Drude behavior at high temperature. This clarifies that T_{coh} is the temperature below which the renormalized ground state (heavy Fermi liquid with a hybridization gap) is fully established.

Inelastic neutron scattering (INS) experiments³ in polycrystalline samples of YbAl_3 have shown that for $T > 50\text{K}$ the magnetic scattering is broad with a characteristic energy of order $E_1 \approx 50\text{meV}$, corresponding to the Kondo temperature,¹ but at low temperature an additional narrow excitation occurs in the INS near $E_2 = 33\text{meV}$. Since this is the same energy as the minimum in the optical conductivity, the excitation lies in the hybridization gap. This peak broadens and weakens on alloying⁴ which fact, taken together with the disappearance of the peak above 50K, means it is a property of the fully coherent ground state. Low temperature peaks with energy corresponding to the hybridization gap also have been observed in Kondo insulators.^{5, 6, 7} Since intermediate valence compounds test our understanding of the correlated electron physics of the Anderson lattice, the characterization of this excitation and its relationship to the peaks seen in the Kondo insulators is an important goal.

To explore the physics of these excitations, and in particular to determine their Q -dependence, we have performed neutron scattering measurements on single crystals of YbAl_3 . The crystals were grown by precipitation from excess aluminum (self-flux method). The experiments were performed at 6K and 100K on the MAPS time-of-flight spectrometer at the ISIS Pulsed Neutron and Muon Facility of the Rutherford Appleton Laboratory. The initial energy was $E_i = 120\text{meV}$. Four crystals, of total mass $\sim 5\text{g}$, were mounted on an aluminum sample holder and co-aligned with \mathbf{k}_i (the incoming beam wavevector) initially parallel the $[1, 0, 0]$ direction; in a second set of measurements we chose $\mathbf{k}_i // [1, 1, 0]$. Unlike the case of a triple-axis spectrometer that can measure a series of single points in the reciprocal space of the crystal to construct a scan over energy transfer with $\mathbf{Q} = (2\pi/a_0) (h, k, l)$ held constant, MAPS employs a large pixellated detector where each individual pixel element detects neutrons on a trajectory through reciprocal space parameterised by the incident energy, E_i , its angle ϕ between the incident \mathbf{k}_i , and final wavevector \mathbf{k}_f and the time-of-flight or energy transfer ΔE . The amalgamation of these simultaneous individual trajectories results in a ‘volume’ of reciprocal space in \mathbf{Q} and ΔE being measured which can be manipulated by software to extract volumes, planes and lines within it.

Fig. 1 shows the scattering averaged over an area ($k = 0.3, l = 0.3$) at three positions in the detector plane. Since YbAl_3 has the Cu_3Au crystal structure (with $a_0 = 4.203\text{\AA}$), the Brillouin zone (BZ) is a simple cube centered at \mathbf{G} and extending ~ 0.5 in reduced (h, k, l) units in all three directions. Hence the averaging in Fig. 1 extends over a considerable fraction of the BZ and thus should approximate a polycrystalline average performed at three values of Q in the extended zone scheme. We assume that the data are

the sum of 1) a background term I_{back} (dotted line) that increases as the average detector angle ϕ increases, and 2) a magnetic term I_{mag} (open circles) that varies with Q as the 4f magnetic form factor. I_{back} and I_{mag} can then be determined uniquely from the low- Q (Fig. 1a) and high- Q (Fig. 1c) data by iterating to self-consistency. The solid line in Fig. 1b, comparing the total scattering at *intermediate- Q* to that predicted by this method, serves as a consistency check on the procedure. Similar assumptions about the variation of the background scattering from small to large detector angle are widely used in studies of polycrystalline intermediate valence compounds.^{3,4} Indeed, the scattering in the interval $10 < \Delta E < 20$ meV is isotropic, suggesting that the background arises primarily from polycrystalline aluminum in the sample environment. The magnetic term can be fit (Fig. 1a, solid line) as the sum of two Lorentzians, the first centered at $E_1 = 51$ meV with a half-width (HWHM) of $G_1 = 21$ meV and the second centered at $E_2 = 33$ meV and with a half-width of $G_2 = 5.3$ meV, which is essentially equal to the instrumental resolution. At 100K we find, using a similar fitting procedure, that the data can be fit as the sum of a background term plus a single Lorentzian at $E_1 = 47$ meV with a halfwidth $G_1 = 29$ meV (not shown here); hence the scattering near E_2 disappears above 50K. These results agree with the earlier results reported for polycrystals.^{3,4}

Fig. 2a shows an intensity map for the projection onto the k - l plane for an interval of energy transfer $E_I = 8$ meV. In this plot, the reduced wavevector h varies with k and l , e.g. for $l = 0$, $h = 1.2$ at $k = 0$ and 1.4 at $k = 1.5$. The cubic symmetry is readily apparent in this plot. Peaks are observed near $(h, 0.5, 0.5)$ where $h(\Delta E = E_I) = 1.2$. These peaks lie essentially at the zone boundary close to the $[0, 1, 1]$ direction. Fig. 2b shows an intensity plot in the ΔE - Q_I plane for an interval $0.4 < k < 0.6$. For $40 < \Delta E < 56$ meV this

shows the same peak as a function of l near $(h(\Delta E), 0.5, 0.5)$ as in Fig. 2a. For $30 < \Delta E < 40$ meV, however, the scattering is basically independent of Q_l . (Under these latter conditions, h varies from 0.85 at $l = 0$ to 1.05 at $l = 1.05$.) A similar plot for $-0.1 < k < 0.1$ shows that the intensity for $30 < \Delta E < 40$ meV is also independent of Q_l ; hence the result does not depend on whether \mathbf{Q} is on the zone boundary, as it is for $k = 0.5$.

To explore the Q -dependence in greater detail, we plot in Fig. 3 the scattering as a function of energy transfer at different positions in momentum space. In these plots, a smaller interval ($k = 0.125, l = 0.125$) of (Q_y, Q_z) is used than in Fig. 1 so that the variation of the scattering within a single Brillouin zone can be determined. The scattering near E_1 shows considerable variation of intensity and lineshape with \mathbf{Q} , as expected on the basis of Fig. 2a. The values of (h, k, l) given in the figure correspond to the value at $\Delta E = E_2 = 33$ meV; hence Fig. 3 shows this peak at key positions in the BZ, including the G point (Fig. 3a), various zone boundary points (Figs. 3b-d) and points in the middle of the BZ (Figs. 3e,f). Plots at other positions in the BZ are very similar. The variation in the position and the magnitude of this peak is small, confirming that the peak at E_2 is essentially independent of \mathbf{Q} .

To demonstrate these contentions in yet another manner, we plot in Fig. 4a the scattering summed over an interval of energy about E_1 and E_2 ; the scattering near E_1 peaks at the zone boundary ($l = 0.5$) but the scattering near E_2 is independent of \mathbf{Q} . In Fig. 4b we remove the background and the $4f$ form factor and plot the magnetic scattering S_{mag} for $l = 0$ and 0.5 integrated over an interval 5 meV near E_1 and E_2 , versus k . The magnetic scattering $S_{mag}(E_1)$ shows a well-defined peak at $\mathbf{Q}_{max} = (2p/a_0)(1.2, 0.5, 0.5)$, but $S_{mag}(E_2)$ is clearly independent of k .

Given the renormalized band structure of Fig.4b, inset, and given that the neutron spectrum reflects the joint density of states (DOS), the interband scattering should give rise to a highly Q -dependent spectrum. The largest intensity should occur for zone boundary \mathbf{Q}_{BZ} , i.e. for scattering from the top of the occupied band to the bottom of the unoccupied band, because the DOS is largest at these locations; the characteristic energy of such scattering should be equal to the indirect gap. Given the results of Figs. 2a and 4, this appears to be the case for the scattering near $E_1 = 50\text{meV}$ for YbAl_3 , so that 50meV is both the Kondo scale and the scale of the indirect gap. The change of lineshape with \mathbf{Q} for the 50meV scattering seen in Fig. 3 is also expected for such scattering, since small \mathbf{Q} preferentially weights larger energy transitions than \mathbf{Q}_{BZ} .

However, apart from the variation with the $4f$ form factor, the scattering near $E_2 = 33\text{meV}$ appears to be independent of \mathbf{Q} , and hence represents a spatially localized excitation. As mentioned above, the energy of the excitation coincides with the deep minimum in the optical conductivity, suggesting that the localized excitation lies in the hybridization gap. Sharp excitations whose energy is in the hybridization gap have been observed at low temperatures in Kondo insulators, such as TmSe ,⁵ SmB_6 ⁶ and YbB_{12} ,⁷ suggesting a common origin for the E_2 excitation in YbAl_3 . This commonality is in accordance with the view that the intermediate valence metals are similar to the Kondo insulators in that the physics is dominated by the hybridization gap, as opposed to the heavy Fermion compounds whose physics is dominated by proximity to a quantum critical point for a magnetic-nonmagnetic transition. However, in the Kondo insulators the hybridization gap excitations are highly Q -dependent; e.g. in TmSe , the intensity is at least a factor of four smaller at zone center than at the zone boundary, and in SmB_6 the

intensity is largest at the zone boundary along the [1, 1, 1] direction and decreases an order of magnitude as Q increases or as the angle of Q with respect to the [1,1,1] direction changes. For CeNiSn⁸ the static susceptibility $\chi'(Q, \omega = 0)$ is independent of Q , but the dynamic susceptibility $\chi''(Q, \omega \neq 0)$ is highly Q -dependent. For YbAl₃ there is no such large variation of intensity of the E_2 peak for different values of Q , including zone center, key zone boundary points and points in the center of the reduced zone (Fig. 3). Hence the excitation differs in an important respect from that seen in the Kondo insulators.

The existence of a spatially localized excitation lends some support to the concept that in heavy Fermion and intermediate valence compounds, localized and itinerant excitations coexist at low temperatures.⁹ However, it should be pointed out that in YbAl₃, it is the interband transitions near $E_I = 50\text{meV}$ which are related most directly to the Kondo impurity scattering. This can be seen from the fact that the pseudo-polycrystalline averages of Fig.1 have characteristic energy 50meV, which is essentially equal to the Kondo energy ($T_K \sim 600\text{-}700\text{K}$) determined from the bulk measurements.¹ The itinerant Fermi liquid excitations, which should occur at very low energies due to scattering close to the Fermi surface and which give rise to the Drude scattering in the optical conductivity, have never been observed by neutron scattering in intermediate valence compounds. The localized excitation at $E_2 = 33\text{meV}$ is neither Fermi liquid scattering nor the Q -dependent remnant of Kondo scattering (i.e. intergap scattering) expected for the Anderson lattice. It is, rather, more in the nature of a local exciton. For example, it might represent an onsite valence excitation into the trivalent ($4f^3$) state. Brandow¹⁰ showed that if such an elementary excitation, which unbinds or unscreens a

local moment at an arbitrary lattice site, is included in a consistent manner with the usual excited states of the Anderson lattice, the two-peak structure of the susceptibility and specific heat can be reproduced. In his treatment, however, the excitation was not derived from the Anderson lattice Hamiltonian but was included in an *ad hoc* manner. It is thus open question whether and how such an excitation can arise in the context of the Anderson lattice. In any case, it is unclear why such an excitation would be localized in the IV metal but Q -dependent in the Kondo insulators. It is also unclear why a local excitation should be so sensitive to alloy disorder.⁴ The E_1 excitation is known⁴ to broaden on alloying; perhaps this broadening, together with the onset of disorder-induced states in the gap, increases the damping of the E_2 excitation.

Work at UC Irvine was supported by the US Department of Energy (DOE) under Grant No. DE-FG03-03ER46036. Work at Argonne National Laboratory was supported by the DOE under Contract No. W-31-109-ENG-38. Work at Los Alamos National Laboratory was also performed under the auspices of the DOE.

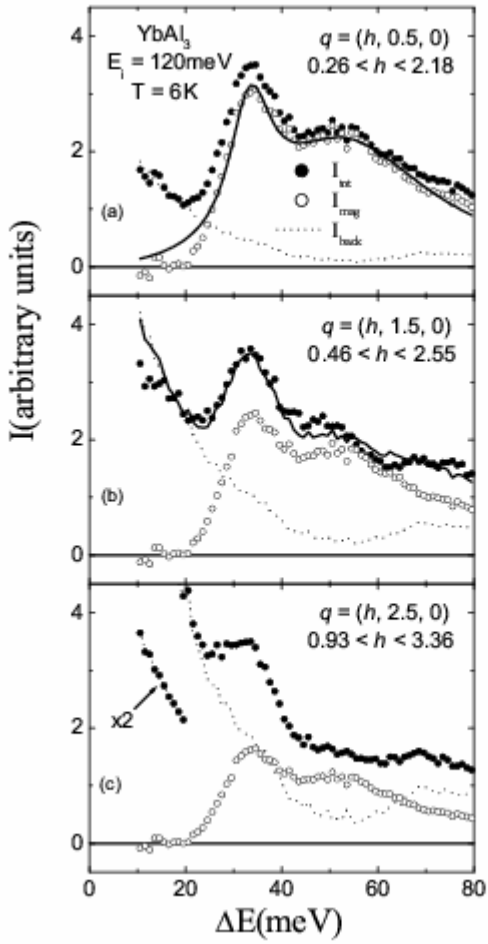


Fig. 1 The scattering intensity (closed circles) versus energy transfer at three values of reduced wavevector k and at $l = 0$; the reduced wavevector h varies approximately linearly with energy transfer between the limits given in each panel. The background scattering (dotted lines) and magnetic scattering (open circles) are determined from the data of a) and b) as described in the text and their sum (solid line) is compared to the data in b) as a consistency check. The solid line in a) is a two-Lorentzian fit to the magnetic scattering (see text).

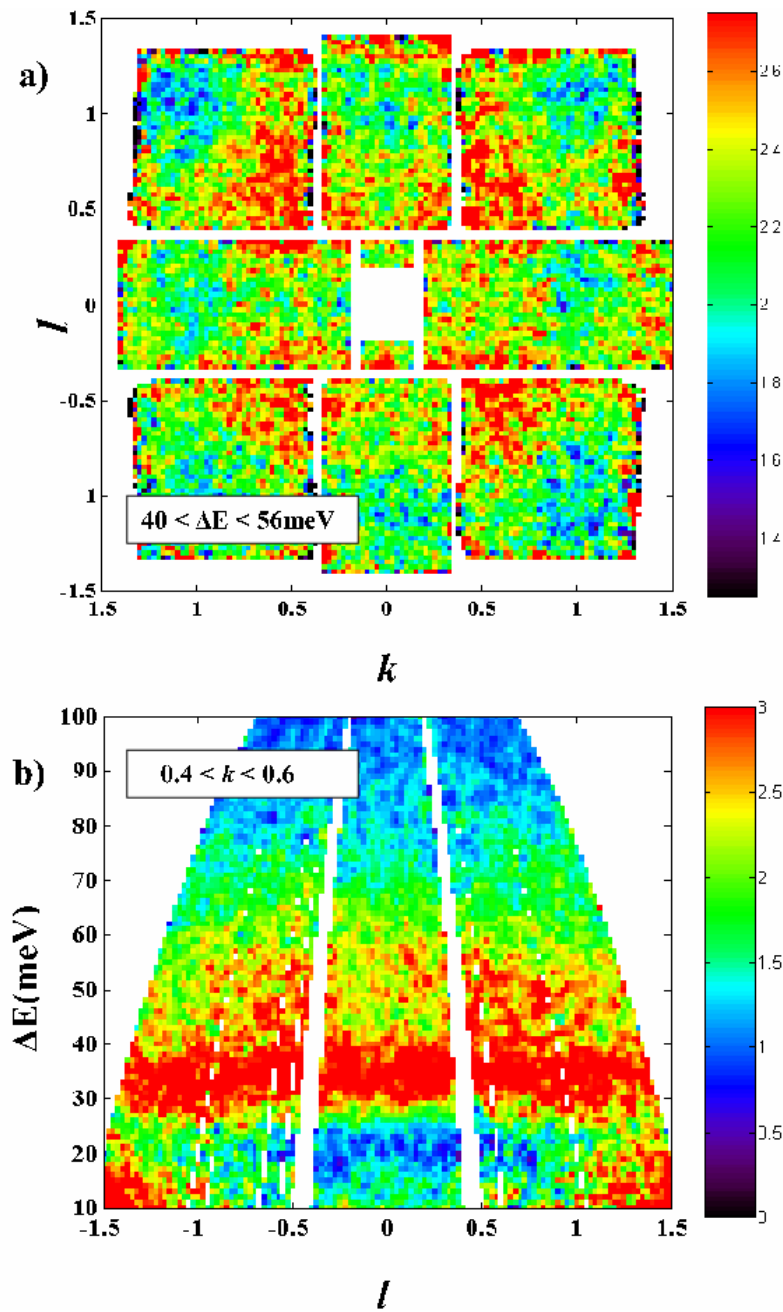


Fig. 2 a) Intensity versus reduced wavevector (k, l) for energy transfers in the range $40 < \Delta E < 56 \text{ meV}$. b) Intensity versus energy transfer ΔE and reduced wavevector l for the component k of reduced wavevector in the range $0.4 < k < 0.6$.

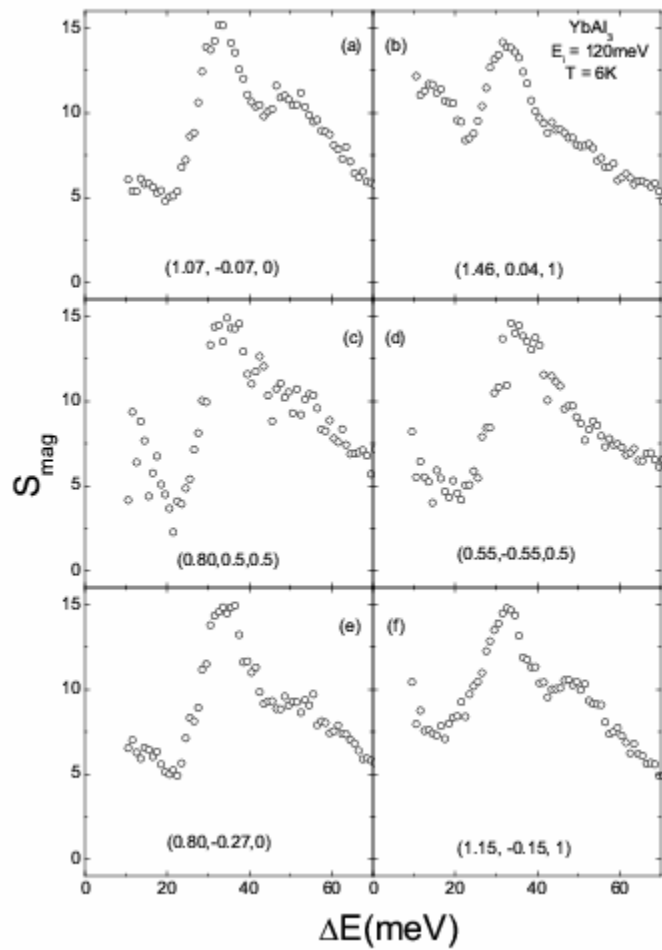


Fig. 3 The scattering intensity in YbAl_3 versus energy transfer at six positions in the detector plane. The reduced wavevectors given in each panel correspond to the value at $\Delta E = E_l = 33 \text{ meV}$.

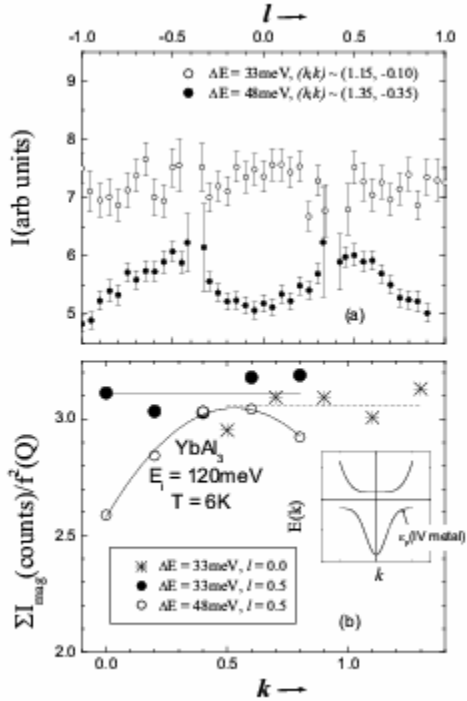


Fig. 4 a) The total scattering near $E_1 = 48\text{meV}$ and $E_2 = 33\text{meV}$ versus reduced wavevector l ; the approximate values of h and k are given in the plot. b) The magnetic scattering for YbAl₃ integrated over an interval $\sim 5\text{meV}$ and versus reduced wavevector k near E_1 for $l = 0.5$, and near for $l = 0$ and 0.5 . Inset: Schematic plot of the renormalized band structure for the Anderson lattice, with a hybridization gap. For IV metals, the Fermi level lies in the high density of states region of the lower band.

¹ A. L. Cornelius, J. M. Lawrence, T. Ebihara, P. S. Riseborough, C. H. Booth, M. F. Hundley, P. G. Pagliuso, J. L. Sarrao, J. D. Thompson, M. H. Jung, A. H. Lacerda, and G. H. Kwei, *Phys. Rev. Lett.* **88**, 117201 (2002).

² H. Okamura, T. Michizawa, T. Nanba, and T. Ebihara, *J. Phys. Soc. Jpn.* **73**, 2045 (2004).

³ A. P. Murani, *Phys. Rev. B* **50**, 9882 (1994).

⁴ R. Osborn, E. A. Goremychkin, I. L. Sashin, and A. P. Murani, *J. Appl. Phys.* **85**, 5344 (1999).

⁵ S. M. Shapiro and B. H. Grier, *Phys. Rev. B* **25**, 1457 (1982).

⁶ P. A. Alekseev, J.-M. Mignot, J. Rossat-Mignod, V. N. Lazukov, I. P. Sadikov, E. S. Konavalova, and Yu. B. Paderno, *J. Phys.: Condens. Matter* **7**, 289 (1995).

⁷ P. A. Alekseev, J.-M. Mignot, K. S. Nemkovski, E. V. Nefedova, N. Yu. Shitsevalova, Yu. B. Paderno, R. I. Bewley, R. S. Eccleston, E. S. Clementyev, V. N. Lazukov, I. P. Sadikov, and N. N. Tiden, *J. Phys.: Condens. Matter* **16**, 2631 (2004).

⁸ T. E. Mason, G. Aeppli, A. P. Ramirez, K. N. Clausen, C. Broholm, N. Stücheli, E. Bucher, and T. T. M. Palstra, *Phys. Rev. Lett.* **69**, 490 (1992).

⁹ S. Nakatsuji, D. Pines and Z. Fisk, *Phys. Rev. Lett.* **892**, 016401 (2004).

¹⁰ B. H. Brandow, *Phys. Rev. B* **37**, 250 (1988).